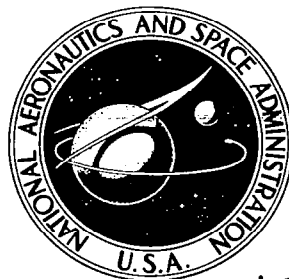


**NASA CONTRACTOR
REPORT**

NASA CR-2732



NASA-CR-52



LOAN COPY: RETURN TO
AFWL TECHNICAL LIBRARY
KIRTLAND AFB, N. M.

**SOME INCONSISTENCIES
OF THE FINITE ELEMENT METHOD
AS APPLIED TO INELASTIC RESPONSE**

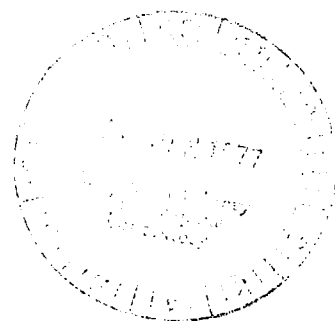
Manohar P. Kamat and Douglas E. Killian

Prepared by

VIRGINIA POLYTECHNIC INSTITUTE AND STATE UNIVERSITY

Blacksburg, Va. 24061

for Langley Research Center



NATIONAL AERONAUTICS AND SPACE ADMINISTRATION • WASHINGTON, D. C. • DECEMBER 1976



0061412

1. Report No. NASA CR-2732		2. Government Accession No.		3. Recipient's Catalog No.	
4. Title and Subtitle SOME INCONSISTENCIES OF THE FINITE ELEMENT METHOD AS APPLIED TO INELASTIC RESPONSE				5. Report Date December 1976	
				6. Performing Organization Code	
7. Author(s) Manohar P. Kamat and Douglas E. Killian				8. Performing Organization Report No. 313635-1	
9. Performing Organization Name and Address Virginia Polytechnic Institute & State University Department of Engineering, Science & Mechanics Blacksburg, VA 24061				10. Work Unit No. 505-02-13-01	
				11. Contract or Grant No. NGR 47-004-114	
12. Sponsoring Agency Name and Address National Aeronautics & Space Administration Washington, DC 20546				13. Type of Report and Period Covered Contractor Report	
				14. Sponsoring Agency Code	
15. Supplementary Notes Langley technical monitor: Robert J. Hayduk Topical report.					
16. Abstract The inadequacy of a two noded beam-column element with a linear axial and a cubic transverse displacement field for inelastic analysis is demonstrated. For complete equilibrium satisfaction in the linear elastic range a three noded beam-column element is shown to be consistent. Next, the sensitivity of the inelastic response to numerical integration of strain energy is examined. Significant differences between the exact and numerical solutions of the inelastic response of a cantilever beam resulting from approximate integration of strain energy are brought out and finally, consequences of this on the nonlinear transient response of structures are considered.					
17. Key Words (Suggested by Author(s)) Inelastic Finite element Nonlinear transient response				18. Distribution Statement Unclassified - Unlimited Subject Category 39	
19. Security Classif. (of this report) Unclassified	20. Security Classif. (of this page) Unclassified	21. No. of Pages 31	22. Price* \$3.75		

CONTENTS

	<u>Page</u>
I. Introduction	1
II. Beam - Column Element	3
III. Sensitivity of Response to Approximations of Energy Estimates	5
IV. Conclusions	11
V. References	12
VI. Tables	13
VII. Figures	15
VIII. Appendix A	24
IX. Appendix B	26

TABLES

1. Comparison of Beam Response for Various Integration Schemes.	13
2. Properties of the Beam on Elastic Supports	14

FIGURES

1a. Two Noded Beam-column Element	15
1b. Three Noded Beam-column Element	15
2a. A Cantilever Beam with Moment at the Tip	16
2b. Stress-Strain Curve (Tension and Compression)	16
3. Strain Distribution over the Beam Cross-Section	17
4. A Solid Cross-Section Beam under an Impulsive Load	18
5. Acceleration-Time Signature of Node 6	19
6. Dissipative Energy versus Time	20
7a. Finite Element Model of a Beam on Elastic Supports	21
7b. Gauss Point Distribution for a Box Section	21
8. Acceleration-Time Signature of Node 3	22
9. Dissipative Energy versus Time	23

I. INTRODUCTION

Nonlinear transient analysis of structures, especially those involving material nonlinearities, are highly complicated even for the uniaxial case with a simple constitutive model. In the case of the beam bending problem for instance, there is a single component of strain along the longitudinal beam axis. This axial strain component is assumed to vary linearly over the cross-section by virtue of the assumption that plane sections remain plane. However, since the stresses are no longer proportional to strains in the inelastic range the distribution of stresses can be quite complex over the cross-section and along the length of the beam. Thus, for a beam which has yielded in a certain region the line of zero stress or strain does not coincide with the centroidal axis in that region. Hence, in general the centroidal axis is not an axis of constant strain for deformations in the inelastic range.

A two-noded beam column element is often used to analyze inelastic response of models built up from such elements in conjunction with other elements. A linear axial displacement field and a cubic transverse displacement field are used in arriving at the stiffness properties of such an element. If the centroidal axis is used as the reference axis, it is not possible to satisfy equilibrium in the inelastic range. The same is true of the linear elastic range, if an axis other than the centroidal axis is used as the reference axis. Hence, a simple linear elastic analysis with an arbitrary reference axis can be used to demonstrate the point under consideration.

Another feature of the nonlinear analysis by the finite element method is the necessity of integrating complex distributions of stresses and strain energy densities over the volume of the element. Because of the

complexity of the integrand and the domain of integration, recourse to numerical schemes like Gaussian quadratures, Newton-Cotes, etc. has to be made in order to obtain approximate estimates of stress resultants and total energies. The number of integration points used over the cross-section and over the length of the beam element determines the degree of approximation. Accordingly approximate estimates of energies yield solutions of varying degrees of accuracy which depend upon the order of the integration scheme used. For an assessment of the quality of such approximate solutions it is necessary that an exact solution to a problem be known. Such a problem along with its accompanying exact solution has been outlined and a rigorous evaluation of the sensitivity of the quasi-static response to the order of the integration scheme is made. For problems, especially those involving transient response, for which no exact solutions can be obtained, only qualitative estimates of sensitivity can be obtained by a comparison of numerical solutions using different orders of integration schemes.

II. BEAM-COLUMN ELEMENT

In this section the two-noded beam-column element of Fig. 1.a will be shown to yield inaccurate results when used to model a beam bending elastically about its centroidal axis, but analyzed with respect to another reference axis. With the finite element formulation in mind the present discussion will be confined to Euler-Bernoulli beams subjected to concentrated shears and moments. For such a beam the total potential energy of deformations is given by

$$\pi = \int_0^l \int_A \frac{E}{2} \left[\frac{du}{dx} - z \frac{d^2w}{dx^2} \right]^2 dAdx - P_1 w(0) - P_2 w(l) - M_1 \frac{dw}{dx}(0) - M_2 \frac{dw}{dx}(l) \quad (1)$$

where u and w are the axial and transverse displacements of the reference axis and z is measured normal to the reference axis. Minimization of π with respect to u and w yields

$$EI \frac{d^4w}{dx^4} - E\bar{z}A \frac{d^3u}{dx^3} = 0 \quad (2)$$

$$EA \frac{d^2u}{dx^2} - E\bar{z}A \frac{d^3w}{dx^3} = 0 \quad (3)$$

as the governing equations (see Appendix A for details). Elimination of u from the above two equations yields the well known equilibrium equation

$$EI_C \frac{d^4w}{dx^4} = 0 \quad (4)$$

where

$$I_C = I - \bar{z}^2 A \quad (5)$$

I_C in Eq. (5) is the moment of inertia of the cross-section about the centroidal axis which is separated from the reference axis by \bar{z} .

Equation (3) integrates to

$$u = \bar{z} \frac{dw}{dx} + c_1 x + c_2 \quad (6)$$

Assume such a beam is to be modeled using the beam-column element of Fig. 1.a. This finite element assumes a cubic transverse displacement of the reference axis. For satisfaction of equilibrium, Eq. (6) requires that the axial displacement vary quadratically over the length of the element. Hence, equilibrium cannot be satisfied by prescribing a linearly varying axial displacement field as is done in the case of the two noded beam element. As an example, a two noded beam element, used to represent a cantilever loaded at its free end with a concentrated transverse load P , yields the following results (see Appendix B for details):

$$u_2 = \bar{z}\theta_2 \quad (7-a)$$

$$\theta_2 = -\frac{Pl^2}{2EI_c} \quad (7-b)$$

$$w_2 = -\frac{Pl^3}{12EI_c} \left(3 + \frac{I_c}{I}\right) \quad (7-c)$$

$$\left. \frac{d^2w}{dx^2} \right|_{x=l} = \frac{Pl}{2EI_c} \left(\frac{I_c}{I} - 1 \right) \quad (7-d)$$

These results are correct only for the case $I = I_c$ i.e., the reference axis for the two noded beam-column element is the centroidal axis.

On the other hand the same cantilever if modeled with a single beam element of Fig. 1.b yields the correct results and ensures a complete satisfaction of equilibrium in keeping with the elementary beam theory.

From this linear elastic example it can be concluded that a three noded beam element is necessary to analyze the inelastic response of structures built up using frame elements, since in general the reference axis is not the neutral axis or an axis of constant axial strain when yielding takes place over portions of the element.

III. SENSITIVITY OF RESPONSE TO APPROXIMATIONS OF ENERGY ESTIMATES

a. Exact Solution:

The exact solution of a quasi-static inelastic beam problem will be developed in order to demonstrate the sensitivity of the response to the order of the integration scheme used in approximate solutions of the problem. Consider the cantilever beam of rectangular cross-section of Fig. 2.a subjected to a bending moment at its tip. The material of the beam is assumed to be linearly elastic--linearly strain hardening as shown in Fig. 2.b. For monotonic loading such a material is conservative and hence the principle of the stationary value of the total potential energy can be used to obtain the governing Euler-Lagrange equations for the beam.

Euler-Bernoulli hypotheses imply that

$$\epsilon(x) = -y \frac{d^2 w(x)}{dx^2} \quad (8)$$

From Fig. 2.b

$$\left. \begin{aligned} \sigma &= E_1 \epsilon \\ &= E_1 \epsilon_y + E_2 (\epsilon - \epsilon_y) \end{aligned} \right\} \begin{array}{l} \text{if } \epsilon \leq \epsilon_y \\ \text{if } \epsilon \geq \epsilon_y \end{array} \quad \begin{array}{l} (9-a) \\ (9-b) \end{array}$$

The total potential energy of the beam of Fig. 2 is given by

$$\pi = \int_{V_1} W_1 dv + \int_{V_2} W_2 dv - M \frac{dw}{dx} \Big|_{x=\ell} \quad (10)$$

where

$$W_1 = \frac{E_1 \epsilon^2}{2} \quad (11-a)$$

$$W_2 = \frac{E_1 \epsilon_y^2}{2} + \frac{E_2 (\epsilon - \epsilon_y)^2}{2} + \sigma_y (\epsilon - \epsilon_y) \quad (11-b)$$

V_1 is the volume of the beam within which the beam is everywhere elastic and V_2 is the volume within which the strain at every point exceeds the yield strain, ϵ_y .

From purely statical considerations it is obvious that the beam of Fig. 2 experiences a constant curvature, $\frac{d^2 w}{dx^2}$ and, hence, d_2 of Fig. 3 is a pure constant and not a function of x . This can be shown to be true by minimizing the total potential energy with respect to, not only w , but also d_2 , assuming a priori that d_2 is a function of x . The Euler-Lagrange equation resulting from the variation of π with respect to w and d_2 implies that the curvature, $\frac{d^2 w}{dx^2}$, and d_2 are both constants.

The two Euler-Lagrange equations

$$-d_2^2 \left[\int_0^l \left(\frac{d^2 w}{dx^2} \right)^2 dx \right] - 2\epsilon_y d_2 \left[\int_0^l \left(\frac{d^2 w}{dx^2} \right) dx \right] - \epsilon_y^2 l = 0 \quad (12)$$

$$\frac{d^4 w}{dx^4} = 0 \quad (13)$$

and the associated boundary conditions

$$w(0) = \frac{dw(0)}{dx} = \frac{d^3 w(l)}{dx^3} = 0 \quad (14-a)$$

and

$$(E_2 - E_1) \epsilon_y b (d_1^2 - d_2^2) + \frac{2b}{3} [E_1 d_2^3 + E_2 (d_1^3 - d_2^3)] \left[\frac{d^2 w(l)}{dx^2} \right] = M \quad (14-b)$$

are the result of the variation of π with respect to d_2 and w .

Equations (13) through (14) are satisfied by

$$w=ax^2 \quad (15)$$

where

$$a = \frac{3}{4d_1} \epsilon_y \frac{\left[\left(\frac{M}{E_1 \epsilon_y b d_1} \right)^2 + \left(1 - \frac{E_2}{E_1} \right) \left\{ 1 - \left(\frac{d_2}{d_1} \right)^2 \right\} \right]}{\left[\left(\frac{d_2}{d_1} \right)^3 + \left(\frac{E_2}{E_1} \right) \left\{ 1 - \left(\frac{d_2}{d_1} \right)^3 \right\} \right]} \quad (16)$$

Use of Eq. (15) into Eq. (12) yields

$$ad_2 = - \frac{\epsilon_y}{2} \quad (17)$$

Substitution of a from Eq. (16) into Eq. (17) yields the cubic equation

$$rp^3 - 3(r+s)p - 2(1-r) = 0 \quad (18)$$

with

$$p = \left(\frac{d_2}{d_1} \right)^2, \quad r = 1 - \frac{E_2}{E_1} \quad \text{and} \quad s = \frac{M}{E_1 \epsilon_y b d_1^2} \quad (19)$$

For any given values of r and s, Eq. (18) can be solved by trial and error to obtain the corresponding value of p. The total strain energy of deformation is then given by

$$U_T = \frac{b \epsilon_y d_1}{3} \left[\{ p^3 + (1-r)(1-p^3) \} (2ad_1)^2 - 3r \epsilon_y (1-p^2) (2ad_1) - 3 \epsilon_y^2 r (1-p) \right] \quad (20)$$

If the beam is unloaded after being loaded into the inelastic range and if it is assumed that unloading takes place elastically then it can be easily verified that the recoverable energy of deformation is given by

$$U_R = E_1 b \epsilon_y d_1 \left[\frac{4}{3} p^3 (ad_1)^2 + r^2 \epsilon_y^2 (1-p) - 2ad_1 \epsilon_y r (1-r)(1-p^2) + \frac{4}{3} (1-r)^2 (1-p^3) (ad_1^2) \right] \quad (21)$$

and the energy dissipated in the process of unloading is

$$U_D = U_T - U_R \quad (22)$$

b. Approximate Numerical Solutions:

Three numerical solutions to the problem just outlined are obtained via the minimization of the total potential energy using the three noded beam elements of Fig. 1.b. and using numerical integration schemes of three different orders for the computation of the strain energy of deformations [1]. The first two schemes use Gaussian quadratures of two different orders in that the beam is divided into two strips in one case and into four strips in the other case. A two point Gaussian quadrature formula is used in each direction (the length and the breadth of the strip). The third scheme is the Newton-Cotes scheme which uses a cubic interpolation with four points in each direction. The details of these schemes can be found in any book on numerical analysis [1]. It must be emphasized however that among integration schemes which imply that the integrand can be approximated by a polynomial of some order the Gaussian quadrature scheme is the most efficient. It is well known for instance that only n Gauss points are sufficient to integrate a polynomial of $(2n-1)$ degree exactly while $(n+1)$ points are necessary to integrate a polynomial of n -th degree exactly with the Newton-Cotes integration scheme.

Table 1 shows a comparison of the exact response with that predicted by the three different integration schemes. Of main interest is the dissipative energy. It is obvious from these results that a very high order quadrature is necessary for a good correlation with the exact solution especially for loads where yielding extends over a major portion of the cross-section of the beam. The higher the value of s in Table 1 the more extensive the yielding.

Such large variations in the estimates of deformations and energies for a quasi-static case suggest that a similar study be made in connection with the nonlinear transient response of structures. Since exact solutions to the nonlinear transient response of structures are virtually nonexistent one has to rely on a comparison between numerical solutions using different integration schemes.

Figure 4 shows the details of a solid cross-section beam clamped at both ends and loaded impulsively at the center by a triangularly varying impulse. The material characteristics of this beam are assumed to be as shown in Fig. 2 with $\sigma_y = 28.96 \times 10^7 \text{ N/m}^2$ and $E_1 = 68.95 \times 10^9 \text{ N/m}^2$ and $(E_2/E_1) \approx 0.4286$. A numerical analysis of the transient response of this beam is performed using direct energy minimization at each time step. For the purposes of the integration of strain energy the two different Gaussian quadrature schemes shown in Fig. 4d are employed.

Figures 5 and 6 bring out quite vividly the differences in the response resulting from the use of the two integration schemes. It must be remarked that the deformation-time plots for the two schemes are very nearly identical and hence are not shown. The same cannot be said of the acceleration or energy plots, however. As regards the acceleration-time plot, at certain instances the accelerations predicted by the two models can be seen to be off by as much as 100%. The nonlinear character of the model coupled with numerical approximations defies predictions of trends in response as evidence by the crossing of the two response curves. The model with 16 Gauss points can, in general, be expected to provide a better estimate of dissipation than the model with 8 Gauss points. It can be seen from Fig. 6 that the model with 16 Gauss points predicts a higher dissipation than the model with 8 Gauss points by as much as 15% over the interval considered. Again, this seems to be a peculiarity of these two models and in general one model which may at any given time predict a dissipation higher than the other may very likely also predict a dissipation lower than the other at another time.

Next the sensitivity of the response of thin-walled frame elements is examined. Such elements can be expected to "tone down" the sensitivity of response, if any, to the order of the integration scheme. Figure 7 shows half the finite element model of a horizontal box beam supported on four uprights and loaded impulsively at the center. The beam and the supports are assumed to be made from the same material the stress-strain curve for which is similar to that of Fig. 2. For the purposes of numerical integration using Gaussian quadratures each wall of the box section is assumed to be divided into rectangular strips extending between the two nodes of a frame element with six degrees of freedom at each node. Table 2 lists the relevant properties of the model shown in Fig. 7. Two different integration schemes are employed - one in which each wall is divided into two strips and another in which the same is divided into four strips. As before a two point Gaussian quadrature formula is used in each direction. In the analysis, the effects of shear deformations are ignored in the interest of simplicity of the constitutive model in the inelastic range. An impulsive load is applied at node 3.

Figure 8 shows the plots of acceleration versus time and Fig. 9 shows the plots of dissipative energy versus time for the two integration schemes. Although the response is very nearly identical in the initial stages the responses for the two cases diverge from each other significantly with the passage of time. As expected the structure is much less sensitive to the order of the integration scheme than the solid beam of Fig. 4. However, it is again evident that no trends can be determined since both integration schemes are only approximate. In fact, it would seem that as a result of the approximations in calculations of the strain energies of deformations upper bound solutions, even for conforming finite element models, are not guaranteed. Thus one scheme may provide a better answer than the other at any given time but the higher order scheme may be expected to give better results overall.

IV. CONCLUSIONS

This study has established the necessity of examining every finite element used for modeling structural behavior in the inelastic range, for consistency of assumptions that will guarantee satisfaction of equilibrium. Furthermore, this study has revealed that structures consisting of frame members wherein numerical integration has to be used for the purposes of evaluating stress resultants or strain energies will be sensitive as regards their accelerations and energy dissipations to the order of the numerical integration scheme used. This sensitivity can be expected to be more pronounced for frame members with solid cross-section in comparison with thin-walled members. This study demonstrates the need for higher order integration schemes for improved quality of response in the nonlinear range. Such higher order integration schemes however, would only make the already expensive numerical analysis of nonlinear response only more so.

V. REFERENCES

1. Zienkiewicz, O. C., "Finite Element Method in Engineering Science," McGraw-Hill Book Company, 1971.

Table 1: Comparison of Beam Response for Various Integration Schemes

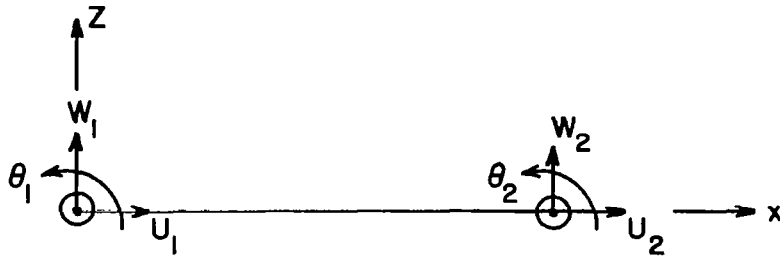
Scheme s	Tip Deflection		Recoverable Energy		Dissipative Energy	
	s_1	s_2	s_1	s_2	s_1	s_2
Exact	1.122489	1.587835	171.19222	269.8933	16.0936	105.2099
Gauss with 32 stress ref. pts/ element	1.13313	1.58667	171.1086	269.8933	19.5555	85.24097
Gauss with 16 stress ref. pts/ element	1.06848	1.63969	170.6667	267.6774	0.5803	109.20314
Newton-cotes with 32 stress ref. pts./element	1.15733	1.53067	159.5500	255.6100	37.0460	87.7340

where $s_1 = -0.8466$, $s_2 = -1.0582$

Table 2. Properties of the Beam on Elastic Supports

Nodes	X m	Y m	Lumped Mass Kilogram	Element	Length m	D ₁ cm	D ₂ cm	t cm
1	0.8001	0.0	-	1	0.7620	3.81	1.463	.0704
2	2.7051	0.0	-	2	0.7620	3.81	1.463	.0704
3	0.0	0.762	0.07793†	3	0.40005	2.9261	7.62	.141
4	0.40005	0.762	0.07793	4	0.40005	2.9261	7.62	.141
5	1.7526	0.762	0.1852	5	0.9525	2.9261	7.62	.141
6	0.8001	0.762	0.14988	6	0.9525	2.9261	7.62	.141
7	2.7051	0.762	0.11138					

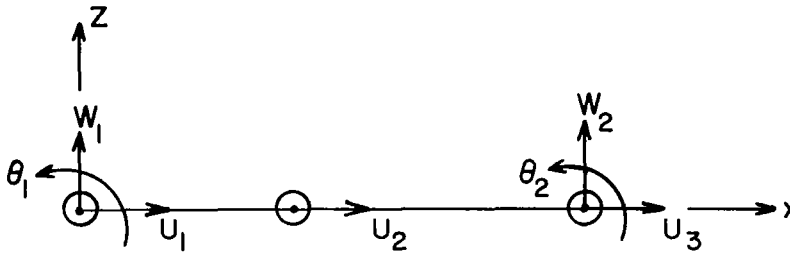
†A non-structural mass of 0.07793 kilogram is assumed to exist at node 3.



$$U(\xi) = (1-\xi)U_1 + \xi U_2, \quad \xi = x/l$$

$$w(\xi) = (1-3\xi^2+2\xi^3)w_1 + l(\xi-2\xi^2+\xi^3)\theta_1 + (3\xi^2-2\xi^3)w_2 + l(-\xi^2+\xi^3)\theta_2$$

Figure 1.a. Two Noded Beam-Column Element



$$U(\xi) = (1-3\xi+2\xi^2)U_1 + (4\xi-4\xi^2)U_2 + (-\xi+2\xi^2)U_3$$

$$w(\xi) = (1-3\xi^2+2\xi^3)w_1 + l(\xi-2\xi^2+\xi^3)\theta_1 + (3\xi^2-2\xi^3)w_2 + l(-\xi^2+\xi^3)\theta_2$$

Figure 1.b. Three Noded Beam-Column Element



Figure 2a. A Cantilever Beam with a Moment at the Tip

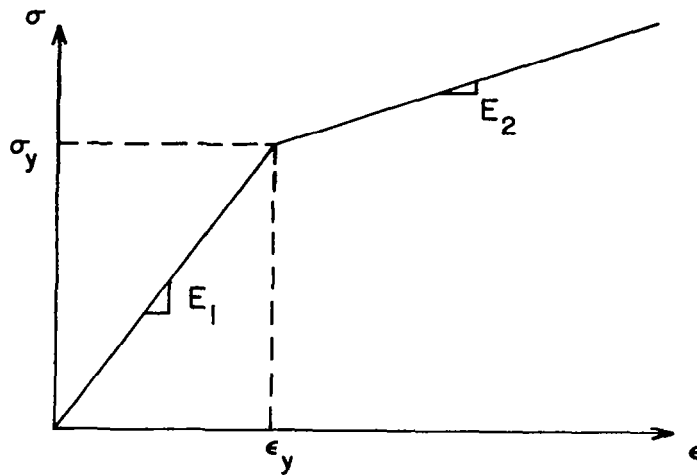


Figure 2b. Stress-Strain Curve (Tension and Compression)

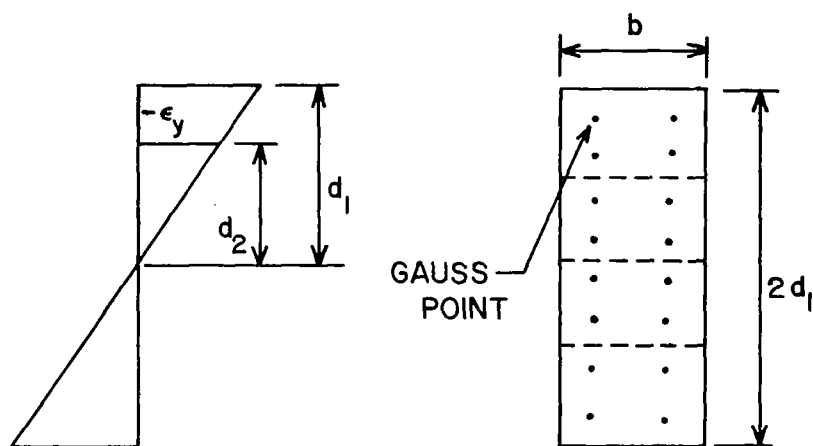
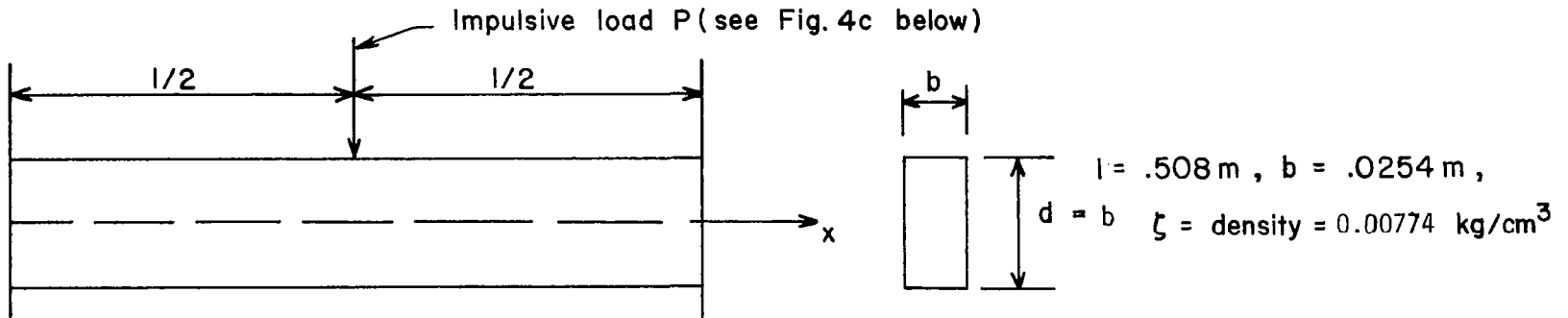


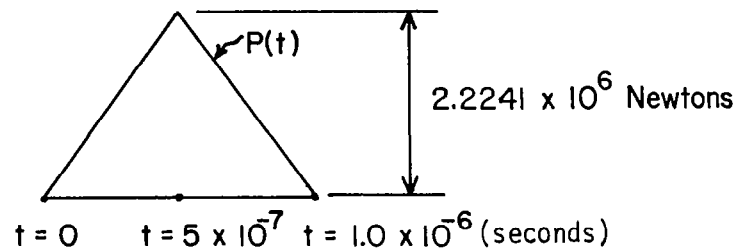
Figure 3. Strain Distribution over the Beam Cross-Section



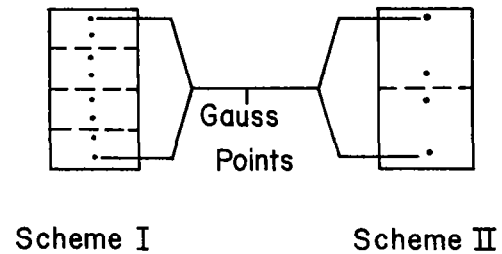
11 Equally spaced nodes — 10 Elements

a. A typical Beam clamped at both ends

b. Beam cross-section



c. Variation of load P



d. Strain energy integration schemes

Figure 4. A Solid Cross-Section Beam Under an Impulsive Load

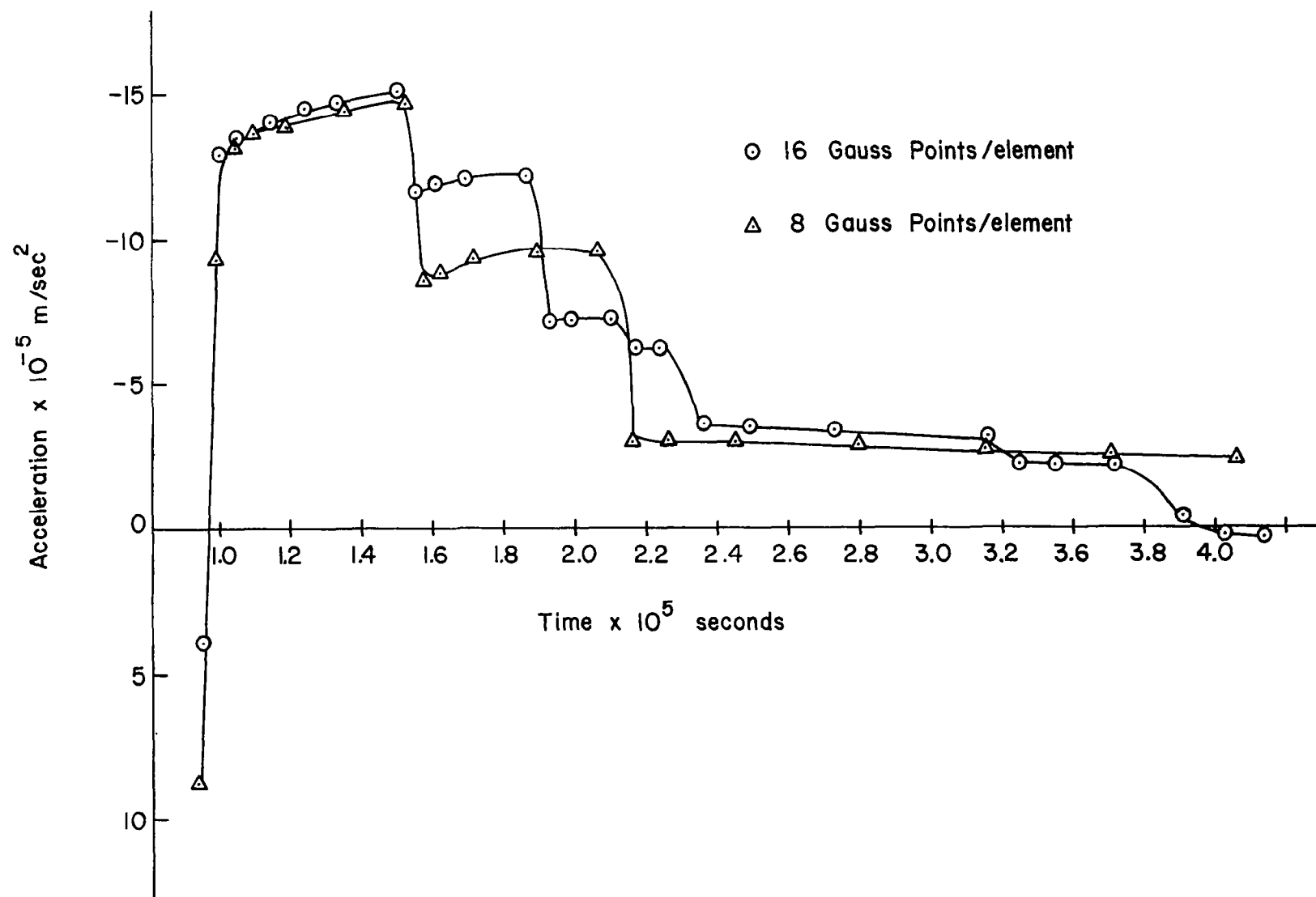


Figure 5. Acceleration-Time Signature of Node 6 (Fig. 4a).

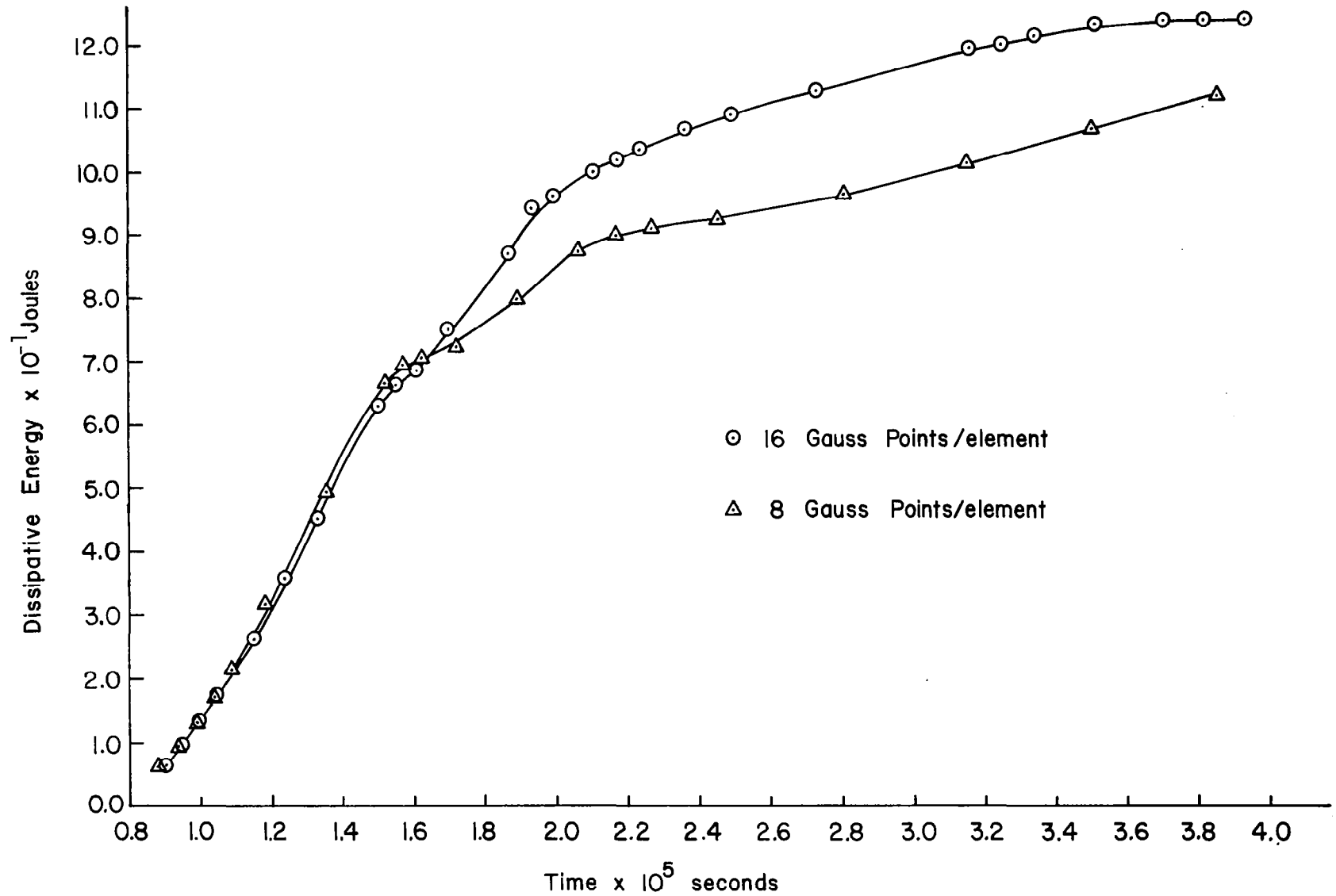


Figure 6. Dissipative Energy Versus Time (Fig. 4a).

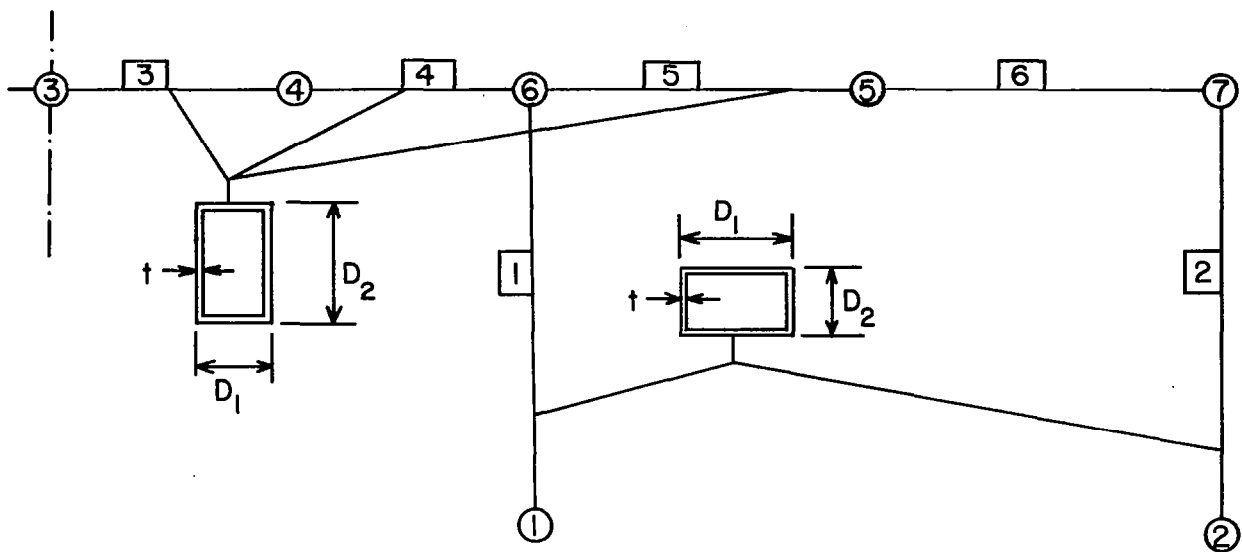


Figure 7.a. Finite Element Model of a Beam on Elastic Supports

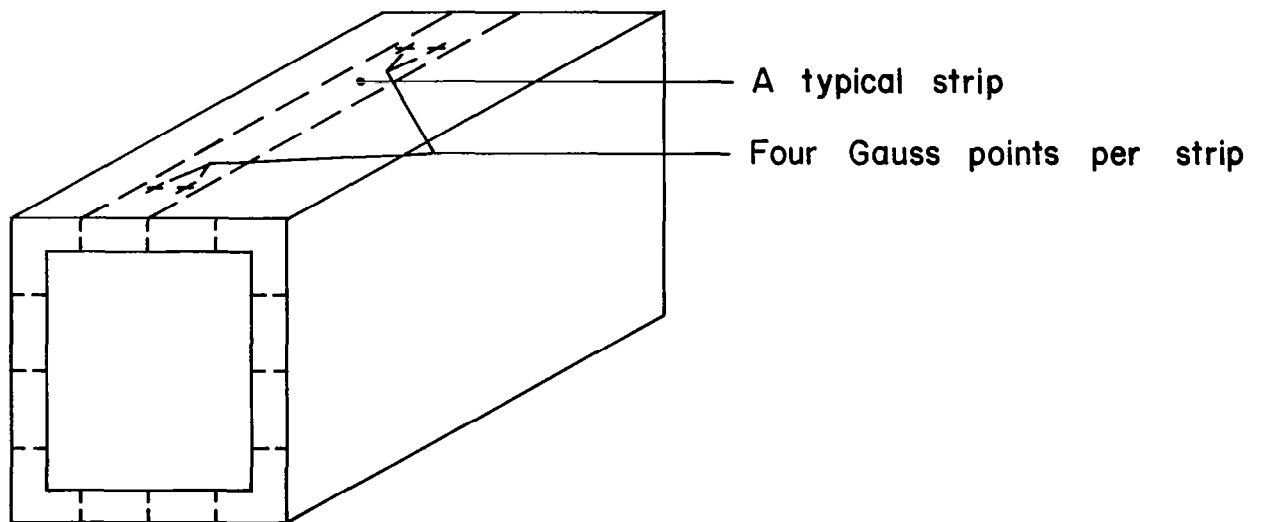


Figure 7.b. Gauss Point Distribution for a Box Section

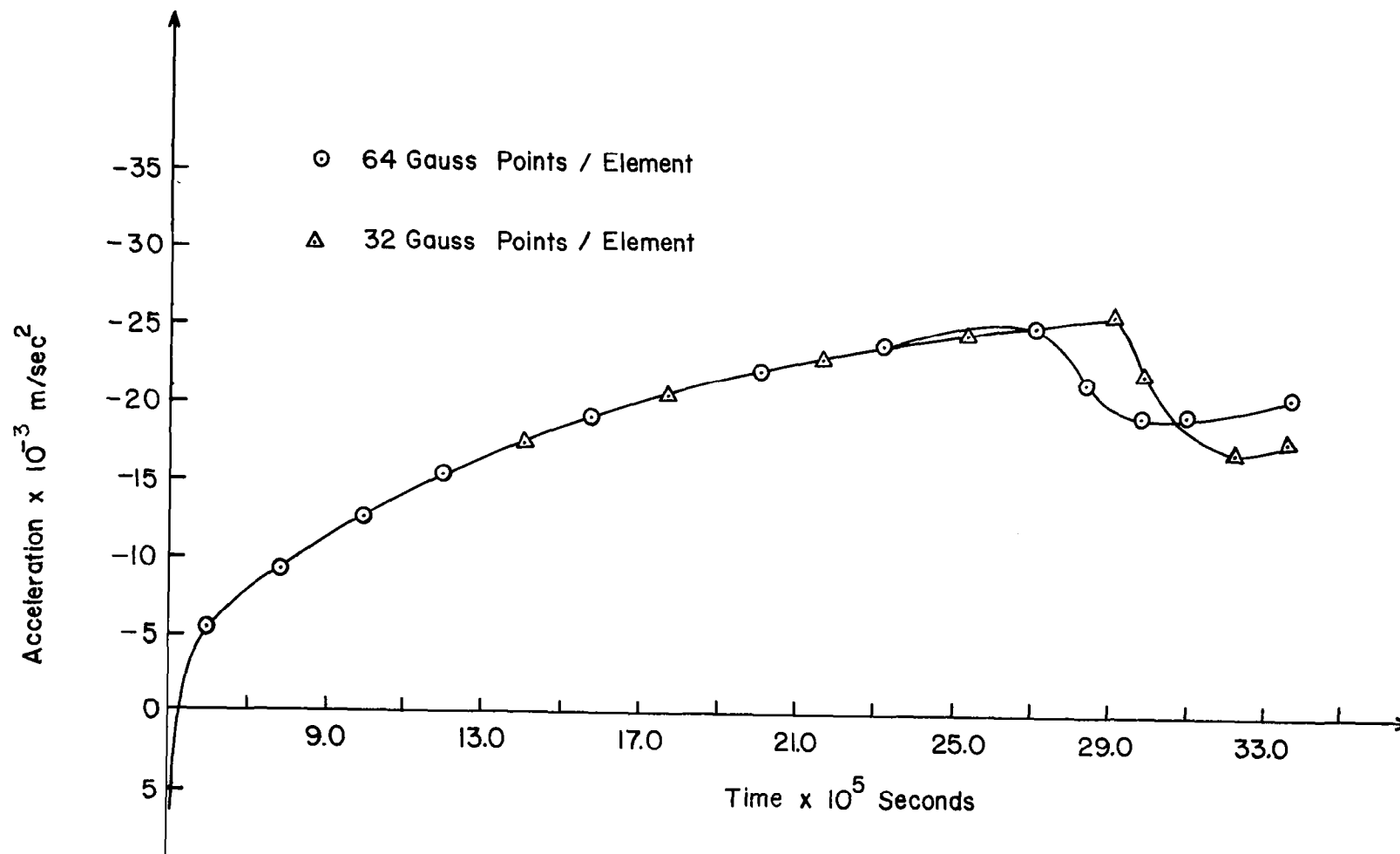


Figure 8. Acceleration-Time Signature of Node 3 (Fig. 7).

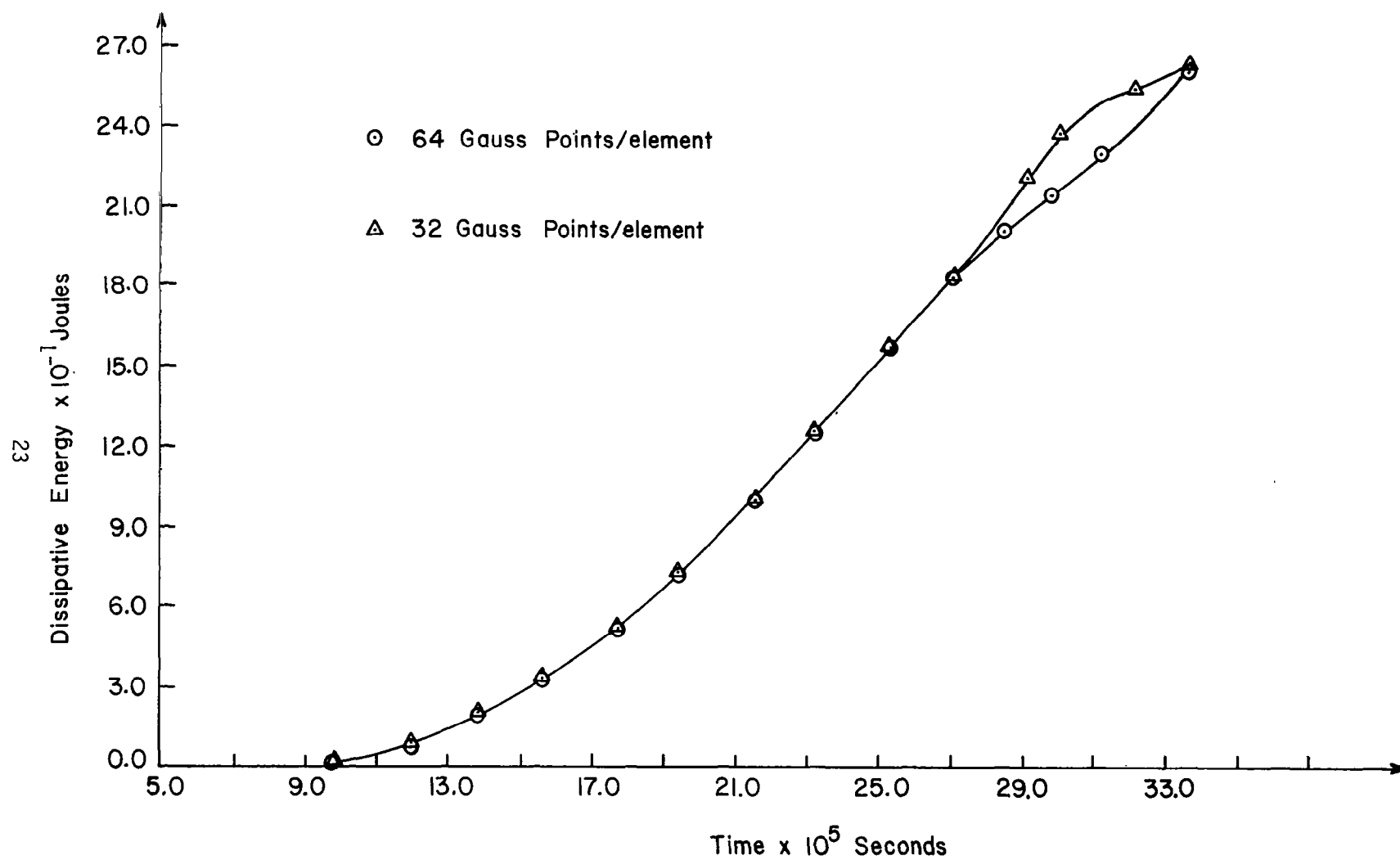


Figure 9. Dissipative Energy Versus Time (Fig. 7).

APPENDIX A

Consider an Euler-Bernoulli beam subjected to end shears and moments. For analyzing the response of this beam, its deformations are referenced with respect to an axis which does not coincide with its centroidal axis around which it bends. This axis is designated as the reference axis. The potential energy expression for such a beam is given by

$$\pi = \int_A \int_0^l \frac{E}{2} \left[\frac{du}{dx} - z \frac{d^2w}{dx^2} \right]^2 dA dx - P_1 w(0) - P_2 w(l) - M_1 \frac{dw}{dx}(0) - M_2 \frac{dw}{dx}(l) \quad (A-1)$$

which upon performing the integration with respect to the area of cross-section reduces to

$$\begin{aligned} \pi = \frac{EA}{2} \int_0^l \left(\frac{du}{dx} \right)^2 dx - E\bar{Z}A \int_0^l \left(\frac{du}{dx} \right) \left(\frac{d^2w}{dx^2} \right) dx + \frac{EI}{2} \int_0^l \left(\frac{d^2w}{dx^2} \right)^2 dx - P_1 w(0) - P_2 w(l) \\ - M_1 \frac{dw(0)}{dx} - M_2 \frac{dw(l)}{dx} \end{aligned} \quad (A-2)$$

where $\bar{Z}A$ and I are respectively the first and the second moments of the area about the reference axis.

Upon requiring that the variation, $\delta\pi$, of the potential energy vanish the necessary Euler-Lagrange equations or the equations of equilibrium of the beam are obtained. Thus,

$$\begin{aligned} \delta\pi = EA \int_0^l \left(\frac{du}{dx} \right) \delta \left(\frac{du}{dx} \right) dx - E\bar{Z}A \int_0^l \left(\frac{du}{dx} \right) \delta \left(\frac{d^2w}{dx^2} \right) dx - E\bar{Z}A \int_0^l \delta \left(\frac{du}{dx} \right) \left(\frac{d^2w}{dx^2} \right) dx \\ + EI \int_0^l \left(\frac{d^2w}{dx^2} \right) \delta \left(\frac{d^2w}{dx^2} \right) dx - P_1 \delta w(0) - P_2 \delta w(l) - M_1 \delta \left(\frac{dw}{dx}(0) \right) - M_2 \delta \left(\frac{dw}{dx}(l) \right) = 0 \end{aligned} \quad (A-3)$$

After integrating by parts the following equations and boundary conditions are obtained.

$$EI \frac{d^4 w}{dx^4} - E\bar{Z}A \frac{d^3 u}{dx^3} = 0 \quad (A-4a)$$

$$EA \frac{d^2 u}{dx^2} - E\bar{Z}A \frac{d^3 w}{dx^3} = 0 \quad (A-4b)$$

Either

$$EA \frac{du(0)}{dx} - E\bar{Z}A \frac{d^2 w(0)}{dx^2} = 0$$

$$EI \frac{d^3 w(0)}{dx^3} - E\bar{Z}A \frac{d^2 u(0)}{dx^2} = P_1$$

$$EI \frac{d^2 w(0)}{dx^2} - E\bar{Z}A \frac{du(0)}{dx} = -M_1$$

$$EA \frac{du(\ell)}{dx} - E\bar{Z}A \frac{d^2 w(\ell)}{dx^2} = 0$$

$$EI \frac{d^3 w(\ell)}{dx^3} - E\bar{Z}A \frac{d^2 u(\ell)}{dx^2} = -P_2$$

$$EI \frac{d^2 w(\ell)}{dx^2} - E\bar{Z}A \frac{du(\ell)}{dx} = M_2$$

or

$$u(0) = u_0^*$$

$$w(0) = w_0^*$$

$$\frac{dw(0)}{dx} = \theta_0^*$$

(A-5a, f)

$$u(\ell) = u_\ell^*$$

$$w(\ell) = w_\ell^*$$

$$\frac{dw(\ell)}{dx} = \theta_\ell^*$$

The starred quantities in the above equations denote prescribed quantities.

APPENDIX B

a. Cantilever Beam Modeled with a Two-Noded Beam Element:

The two noded beam-column element of Fig. 1.a. is used to model a cantilever beam subjected to a load P at its free end. The potential energy for such a beam is given by Eq. (A-1) with $P_1=M_1=M_2=0$ and $P_2=-P$. It can be easily verified that the substitution of expressions for $u(\xi)$ and $w(\xi)$ from Fig. 1.a. into this potential energy expression yields

$$\begin{aligned} \pi = & \frac{EA}{2\ell} [u_1^2 - 2u_1u_2 + u_2^2] - \frac{EA\bar{Z}}{\ell} (u_2 - u_1)(\theta_2 - \theta_1) \\ & + \frac{EI}{2\ell} [12w_1^2 + 12w_1\theta_1\ell - 24w_1w_2 + 12w_1\theta_2\ell + 4\theta_1^2\ell^2 - 12w_2\theta_1\ell \\ & + 4\theta_1\theta_2\ell^2 + 12w_2^2 - 12w_2\theta_2\ell + 4\theta_2^2\ell^2] + Pw_2 \end{aligned} \quad (B-1)$$

Upon requiring that the variation of π with respect to the nodal variables u_1 , u_2 , w_1 , w_2 , and θ_1 , θ_2 be zero the following equations are obtained.

Either

$$\frac{EA}{\ell}(u_1 - u_2) + \frac{E\bar{Z}A}{\ell}(\theta_2 - \theta_1) = 0$$

$$\frac{EA}{\ell}(u_2 - u_1) + \frac{E\bar{Z}A}{\ell}(\theta_1 - \theta_2) = 0$$

$$\frac{EI}{\ell} [12(w_1 - w_2) + 6\ell(\theta_1 - \theta_2)] = 0$$

or

$$u_1 = u_1^*$$

$$u_2 = u_2^*$$

$$w_1 = w_1^*$$

Either

or

$$\frac{EI}{\ell^3} [12(w_2 - w_1) - 6\ell(\theta_1 + \theta_2)] + P = 0$$

$$w_2 = w_2^*$$

(B-2a, f)

$$\frac{EZA}{\ell} (u_2 - u_1) + \frac{EI}{\ell^2} [6(w_1 - w_2) + 2\ell(2\theta_1 + \theta_2)] = 0$$

$$\theta_1 = \theta_1^*$$

$$\frac{EZA}{\ell} (u_1 - u_2) + \frac{EI}{\ell^2} [6(w_1 - w_2) + 2\ell(\theta_1 + 2\theta_2)] = 0$$

$$\theta_2 = \theta_2^*$$

Since, for the cantilever beam the nodal displacements u_1 , w_1 and θ_1 are all prescribed to be zero the three equations corresponding to unknown displacements u_2 , w_2 and θ_2 simplify to

$$u_2 = \bar{Z}\theta_2$$

$$\frac{EI}{\ell^3} (12w_2 - 6\theta_2\ell) + P = 0 \quad (B-3a, c)$$

$$-\frac{EZA}{\ell} u_2 + \frac{EI}{\ell^2} (-6w_2 + 4\theta_2\ell) = 0$$

The above three equations when solved simultaneously yield the following results

$$\begin{aligned} u_2 &= -\bar{Z} \left(\frac{P\ell^2}{2EI_c} \right) \\ w_2 &= -\frac{P\ell^3}{12I_c} \left(3 + \frac{I_c}{I} \right) \\ \theta_2 &= -\frac{P\ell^2}{2EI_c} \end{aligned} \quad (B-4a, c)$$

where $I_c = I - A\bar{Z}^2$.

Furthermore, $\frac{d^2w}{dx^2}$ at the free end (i.e. at $x=\ell$) which is proportional to the bending moment at the free end can now be evaluated to be

$$\frac{d^2w(\ell)}{dx^2} = -\frac{P\ell}{2EI_c} \left(\frac{I_c}{I} - 1 \right) \quad (B-4d)$$

Clearly, the above results reduce to the correct strength of materials results if $I_c = I$ which is to say the reference axis coincides with the centroidal axis.

b. Cantilever Beam Modeled with a Three-Noded Beam Element:

The expression for the potential energy in this case becomes

$$\begin{aligned} \pi = & \frac{EA}{2\ell} \left[\frac{7}{3} u_1^2 + \frac{16}{3} u_2^2 + \frac{7}{3} u_3^2 - \frac{16}{3} u_1 u_2 + \frac{2}{3} u_1 u_3 - \frac{16}{3} u_2 u_3 \right] \\ & - \frac{E\bar{Z}A}{\ell^2} \left[4u_1 w_1 - 8u_2 w_1 + 4u_3 w_1 + 3u_1 \theta_1 \ell - 4u_2 \theta_1 \ell + u_3 \theta_1 \ell - 4u_1 w_2 + 8u_2 w_2 \right. \\ & \left. - 4u_3 w_2 + u_1 \theta_2 \ell - 4u_2 \theta_2 \ell + 3u_3 \theta_2 \ell \right] \\ & + \frac{EI}{2\ell^3} \left[12w_1^2 + 12w_1 \theta_1 \ell - 24w_1 w_2 + 12w_1 \theta_2 \ell + 4\theta_1^2 \ell^2 - 12w_2 \theta_1 \ell + 4\theta_1 \theta_2 \ell^2 \right. \\ & \left. + 12w_2^2 - 12w_2 \theta_2 \ell + 4\theta_2^2 \ell^2 \right] + Pw_2 \end{aligned} \quad (B-5)$$

Upon requiring that the variation of π with respect to the nodal variables u_1, u_2, u_3, w_1, w_2 and θ_1, θ_2 be zero the equations corresponding to the unknown variables u_2, u_3, w_2 and θ_2 are

$$u_2: \frac{EA}{\ell} (16u_2 - \frac{8}{3}u_3) - \frac{E\bar{Z}A}{\ell^2} (8w_2 - 4\theta_2\ell) = 0$$

$$u_3: \frac{EA}{\ell} (-\frac{8}{3}u_2 + \frac{7}{3}u_3) - \frac{E\bar{Z}A}{\ell^2} (-4w_2 + 3\theta_2\ell) = 0$$

(B-6a,d)

$$w_2: -\frac{E\bar{Z}A}{\ell^2} (8u_2 - 4u_3) + \frac{EI}{\ell^3} (12w_2 - 6\theta_2\ell) + P = 0$$

$$\theta_2: -\frac{E\bar{Z}A}{\ell} (-4u_2 + 3u_3) + \frac{EI}{\ell^2} (-6w_2 + 4\theta_2\ell) = 0$$

Simultaneous solution of these equations yields

$$u_3 = -\bar{Z} \left(\frac{p\ell^2}{2EI_c} \right)$$

$$u_2 = -\bar{Z} \left(\frac{3p\ell^2}{8EI_c} \right)$$

(B-7a,d)

$$w_2 = -\frac{p\ell^3}{3EI_c}$$

$$\theta_2 = -\frac{p\ell^2}{2EI_c}$$

These are identical with the well known strength of materials results.